Human Molecular Genetics, 2000, Vol. 9, No. 13 **1957–1966**

CAG tract of *MJD-1* may be prone to frameshifts causing polyalanine accumulation

Claudia Gaspar[+], Merhdad Jannatipour[+], Patrick Dion, Janet Laganière, Jorge Sequeiros[1], Bernard Brais[§] and Guy A. Rouleau[¶]

Centre for Research in Neurosciences, McGill University, and the Montreal General Hospital, 1650 Cedar Avenue, Montréal, Québec H3G 1A4, Canada and [1]Laboratório Genética Médica, ICBAS and UnIGENe, IBMC, Universidade do Porto, Porto, Portugal

Received 30 March 2000; Revised and Accepted 19 June 2000

Machado–Joseph disease (MJD) is one of several disorders caused by the expansion of a coding CAG repeat (exp-CAG). The presence of intranuclear inclusions (INIs) in patients and cellular models of exp-CAG-associated diseases has lead to a nuclear toxicity model. Similar INIs are found in oculopharyngeal muscular dystrophy, which is caused by a short expansion of an alanine-encoding GCG repeat. Here we propose that transcriptional or translational frameshifts occurring within expanded CAG tracts result in the production and accumulation of polyalanine-containing mutant proteins. We hypothesize that these alanine polymers deposit in cells forming INIs and may contribute to nuclear toxicity. We show evidence that supports our hypothesis in lymphoblast cells from MJD patients, as well as in pontine neurons of MJD brain and in *in vitro* cell culture models of the disease. We also provide evidence that alanine polymers alone are harmful to cells and predict that a similar pathogenic mechanism may occur in the other CAG repeat disorders.

INTRODUCTION

Coding CAG triplet repeat expansions cause several neurodegenerative disorders, including Machado–Joseph disease (MJD) (1,2). The presence of intranuclear filamentous inclusions (INIs) containing expanded protein in MJD, as well as in other expanded CAG repeat (exp-CAG) disorders, have lead to a nuclear toxicity model (3–7). Similar INIs are found in oculopharyngeal muscular dystrophy (OPMD) (8), which is caused by short expansions of a polyalanine (polyAla)-encoding GCG tract in the *PABP2* gene (8). In contrast to the CAG repeat disorders, where expansions frequently involve the addition of 20 or more codons, very small GCG expansions (exp-GCG) of two to seven additional codons are seen in dominant OPMD, suggesting that polyalanine tracts are prone to aggregation and may be very toxic (8). This contention is supported by the observation that polyAla peptides containing more than nine alanines in a row form β-pleated sheet fibrillar macromolecules spontaneously *in vitro* (9), which in turn are extremely resistant to chemical and enzymatic degradation (10).

A frameshift error occurring within a CAG tract could result in the alternate alanine-encoding GCA frame. In fact, many authors have reported frameshifts at the level of transcription or translation. The observation of transcriptional errors of the β-amyloid precursor protein and ubiquitin-B in Alzheimer's disease (11), and apoB86 (12), supports the existence of such errors, and their role in disease pathogenesis. Translational errors have also been shown to occur and may be the basis for the formation of frameshifted proteins (13). The occurrence of +2 frameshifts in exp-CAG would lead to a GCA alanine-encoding frame resulting in proteins containing large stretches of polyAla, perhaps much larger than the 12–17 alanines seen in dominant OPMD.

The presence of INIs in both exp-CAG and exp-GCG associated disorders, the relatively short alanine polymers needed for toxicity in OPMD, and the physical properties of these homopolymers, led us to predict that polyAla may accumulate as intranuclear protein aggregates in these disorders. We therefore hypothesize that: (i) rare transcriptional or translational frameshifts in large CAG stretches result in new reading frames with formation of a hybrid protein containing a mixed polyglutamine/polyalanine tract; (ii) the resultant polyAla peptides accumulate in INIs; and (iii) polyAla peptides are toxic to cells.

Here we show that an antiserum raised against the hypothetical C-terminus of the predicted polyAla-containing frameshifted ataxin-3 protein (MJD-Ala) detects the frameshifted species in lymphoblastoid cells from MJD patients with large CAG tracts as insoluble macromolecules on western blots, and as INIs by immunocytochemistry. Frameshifted species were also present in INIs in pontine neurons of MJD brain. Transfection of COS-7 cells with full-length *MJD-1* fused to the enhanced green fluorescent protein (*EGFP*) gene in the alternative polyAla reading frame leads to EGFP accumulation preferentially when the CAG tract is expanded. We also demonstrate that long CAG repeats are prone to frameshifts that result in accumulation of the predicted polyAla-containing inclusions. Transfection of

[+]These authors contributed equally to this work
[§]Present address: Centre de recherche du CHUM, Campus Notre-Dame, Université de Montréal, 1560 rue Sherbrooke est, Montréal, Québec H2L 4M1, Canada
[¶]To whom correspondence should be addressed. Tel: +1 514 934 8094; Fax: 514 934 8265; Email: mi32@musica.mcgill.ca

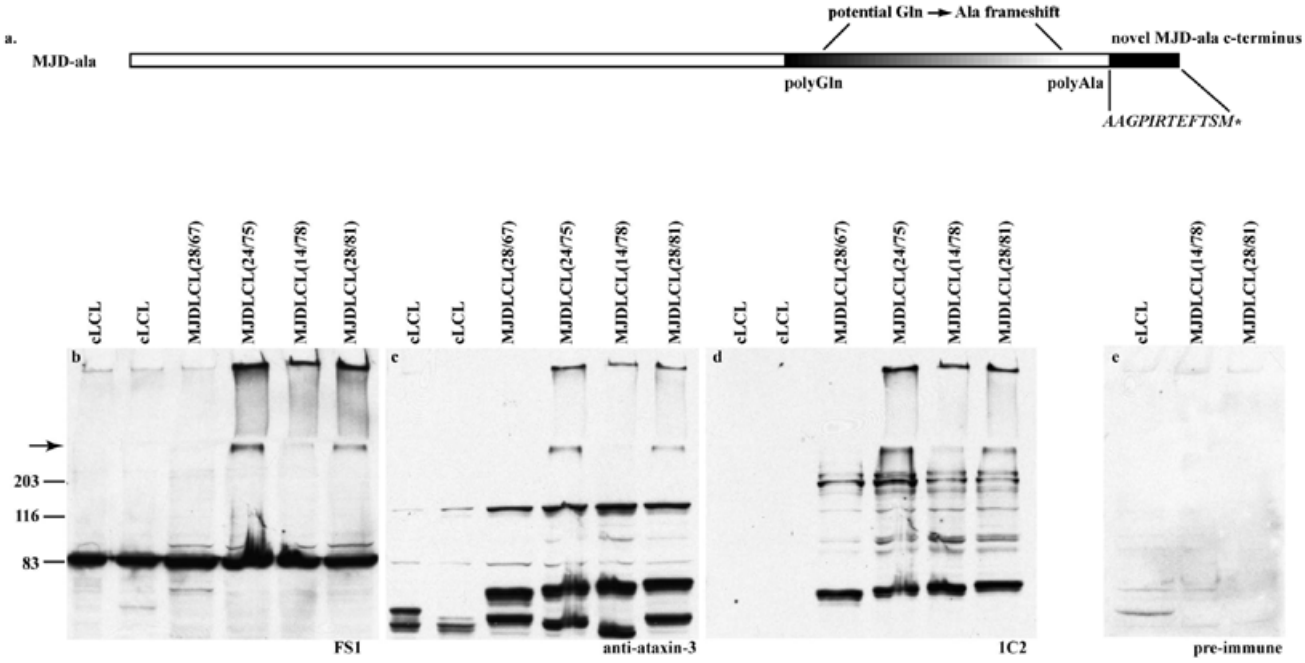

Figure 1. Western blot analysis of lymphoblastoid cells from controls and MJD patients. (**a**) Schematic representation of the MJD-Ala protein that results from a frameshift in the CAG tract showing the new C-terminus (italicized; used to raise the FS1 and FS2 antibodies). (b–e) Western blots of two control lymphoblastoid cell lines (cLCL) and four MJD lymphoblastoid cell lines (MJDLCL) immunoprobed with FS1 (**b**), anti-ataxin-3 (**c**), 1C2 (**d**) and FS1 pre-immune serum (**e**). The arrow indicates the threshold between stacking and resolving portions of the gel. (b)–(d) represent serial probing of a single membrane.

COS-7 cells with mutated *MJD-1* constructs containing alanine-coding GCA stretches results in a more severe phenotype compared with their CAG counterparts. Furthermore, transfected polyAla-encoding GCA stretches alone are damaging and form aggregates.

RESULTS

Frameshifts occur in CAG tracts resulting in polyalanine-containing proteins

Two immunopurified polyclonal antisera were raised against a synthetic peptide corresponding to the last 12 amino acids predicted to result from polyAla tract-producing frameshifts within the CAG repeat of the *MJD-1* gene (FS1 and FS2) (Fig. 1a). This new amino acid sequence has no homology to any known protein. Both antisera detected high molecular weight aggregates in the stacking gels in western blots of total lymphoblast protein from three MJD cases (Fig. 1b). In the two controls and in the MJD patient with the shortest $(CAG)_{67}$ repeat, no aggregates were observed (Fig. 1b). Both FS antibodies also recognize, in all samples, an 83 kDa protein of unknown origin. In order to test whether the signal detected in the stacking gels was the putative MJD-Ala protein, we probed the same blots with antisera raised against MJD protein epitopes (anti-ataxin-3; Fig. 1c) (14) and against polyGln domains (1C2; Fig. 1d) (15). These results are compatible with the presence of the predicted hybrid protein in the stacking gel. An anti-ubiquitin polyclonal antibody also detected the accumulations (data not shown), which is consistent with previous reports (3,6,16–18). These accumulations are compatible with those reported by Paulson *et al.* (3) who studied cells expressing mutant CAG tract expanded *MJD-1* using an antibody raised against the expressed ataxin-3 fusion proteins.

To test whether the MJD-Ala protein accumulates in nuclei we performed immunocytochemistry on lymphoblasts from four controls and three MJD patients. As Figure 2 depicts, FS1-positive INIs are observed in MJD cell lines and not in controls (Fig. 2a and b). Similar to the western blot results, the anti-ubiquitin antibody (Fig. 2c and d) and the anti-ataxin-3 antibody (data not shown) also detect INIs in MJD cell lines.

In an attempt to show the presence of the frameshifted species in affected MJD brain regions, we performed immunohistochemical FS1 and anti-ubiquitin staining in diseased and control pons, a region known to be affected in MJD (Fig. 3). Both antibodies stain intranuclear structures in neurons of this MJD brain area (Fig. 3a and c), whereas pontine neurons in control brain have no INIs (Fig. 3b and d). In immunofluorescence studies, we show that the frameshifted product colocalizes with ubiquitin in INIs of pontine neurons (Fig. 3e–j), suggesting that the intranuclear structures detected by both antibodies are the same.

Frameshifts into alanine frame occur preferentially with expanded CAG tracts

To test whether frameshifts producing GCA/polyAla occur preferentially within expanded CAG tracts, we designed an *in vitro* system to examine the effect of CAG repeat length on the frequency of frameshifts. COS-7 cells were transfected with constructs bearing the full-length *MJD-1* sequence with either a $(CAG)_{14}$, $(CAG)_{37}$ or $(CAG)_{82}$ repeat fused out of frame to the *EGFP* gene and driven by the cytomegalovirus promoter (Figs 4 and 5a). We predicted that frameshifts would occur with all CAG tracts but more frequently within larger repeats.

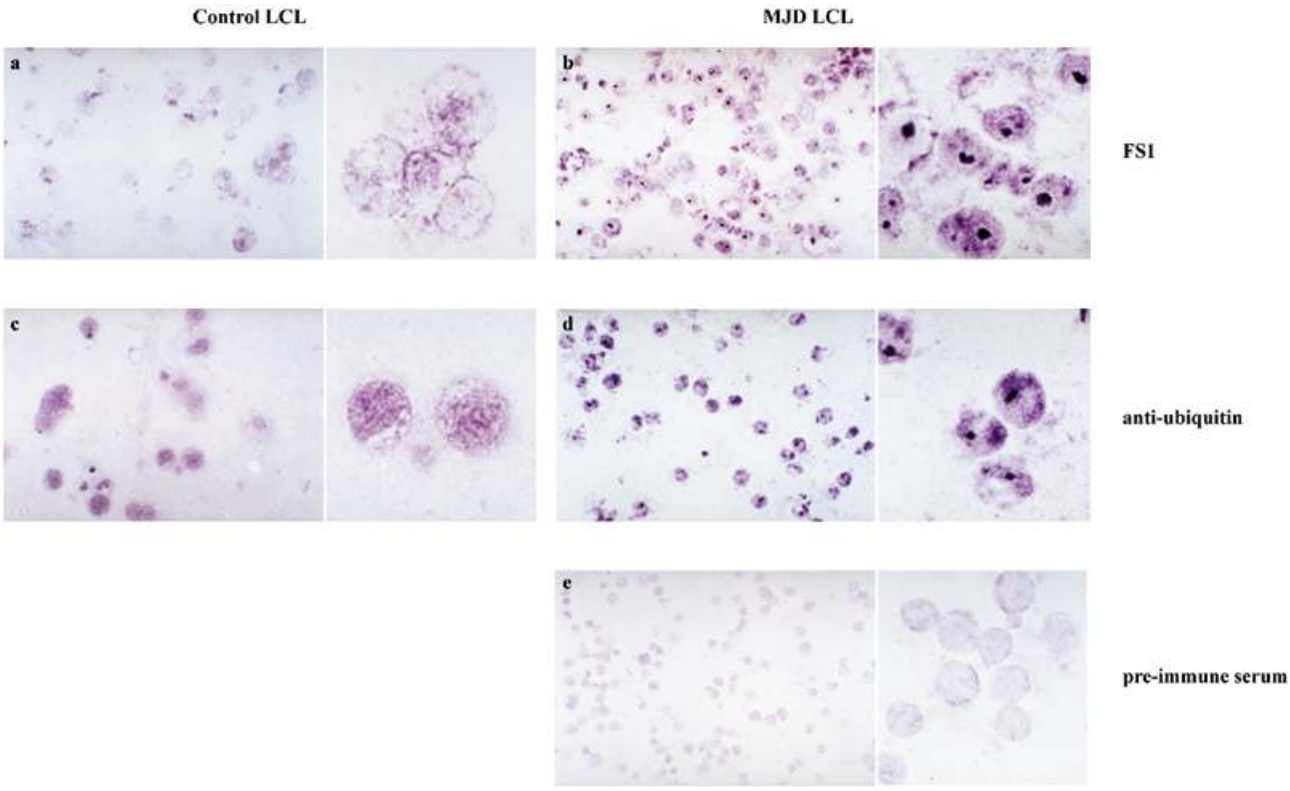

Figure 2. Immunocytochemical detection of intranuclear deposits in lymphoblastoid cells. Immunocytochemistry of control LCL versus MJD LCL: absence of INIs in control LCL probed with FS1 (**a**), with anti-ubiquitin (**c**), and detection of INIs in MJD LCL with FS1 (**b**) and anti-ubiquitin (**d**). (**e**) Immuno-detection of MJD LCL with FS1 pre-immune serum. For all panels, the magnification before publication is 400× (left) and 1000× (right). These results have been replicated in three separate experiments.

The pMJD1, pMJD2 and pMJD3 constructs would yield EGFP-containing fusion proteins only if a frameshift occurs and produces the GCA/polyAla reading frame and the MJD-Ala protein. At 72 h, cells transfected with pMJD2 and, especially pMJD3, showed green fluorescence (Fig. 5c–e). Green fluorescence was observed within 24 h in the positive control cells transfected with the pEGFP-N1 vector alone or pMJD4 construct, where the *EGFP* coding sequence was in the glutamine frame in *MJD-1* (Fig. 5f and g). At 96 h, and at higher magnification, frequent EGFP-positive perinuclear inclusions were observed in cells transfected with the pMJD3 construct (82 CAGs) but not in the construct with 14 CAGs, and rarely in cells transfected with the 37 CAG construct (Fig. 5h). These perinuclear inclusions are similar to those found in cell culture models of MJD, as well as other CAG tract disorders, such as Huntington's disease (3,19).

Western blots of protein extracted from the transfected cells were probed to confirm this interpretation (Fig. 5i–n). Whereas 1C2 detects only the expanded MJD gene products bearing either 37 or 82 polyglutamine repeats in cells transfected with pMJD2 and pMJD3, respectively (Fig. 5j), anti-ataxin-3 detects all three different size polyglutamine tract-containing gene products (Fig. 5k), as expected. With both antibodies we detected protein accumulation in the wells for pMJD3 and pMJD4. Overexposure of blots in Figure 5j and k (Fig. 5m and n, respectively) reveals a band corresponding to the size of ataxin-3 fused to EGFP, showing that some frameshifted product migrates into the gel. The bands detected by 1C2 and anti-ataxin-3 for pMJD4, corresponding to the size of ataxin-3 alone, probably result from cleavage of the hybrid protein to generate ataxin-3 and EGFP. This is supported by the results obtained by probing the blots with the anti-GFP antibody (Fig. 5i), where normal size EGFP is detected. In order to further determine the nature of the accumulated protein seen for pMJD3, we modified the pMJD1 and pMJD3 constructs by adding epitopes for FS1 and hemagglutinin (HA) in the alanine frame (pMJD5 and pMJD6; Fig. 4). Western blots of cells transfected with these constructs were probed with anti-HA. We detected no signal for the 14 CAG-bearing pMJD5 construct, but a band corresponding to aggregated protein was detected at the top of the gel for pMJD6, showing that with 82 repeats frameshifts are occurring (Fig. 5l). The absence of a band corresponding to the predicted size of the ataxin-3/HA protein indicates that all frameshifted protein is accumulating as insoluble aggregates. These experiments further demonstrate that frameshifts do occur and suggest that their frequency increases with the size of the CAG repeat.

Polyalanine-containing proteins are present in aggregates and are harmful to transfected COS-7 cells in a time-dependent manner

We have shown that frameshifting into the alternate alanine frame occurs *in vitro* and *in vivo*. To determine whether these products are toxic or are simply harmless byproducts with no real consequences to the cell, we designed a new set of *MJD-1*

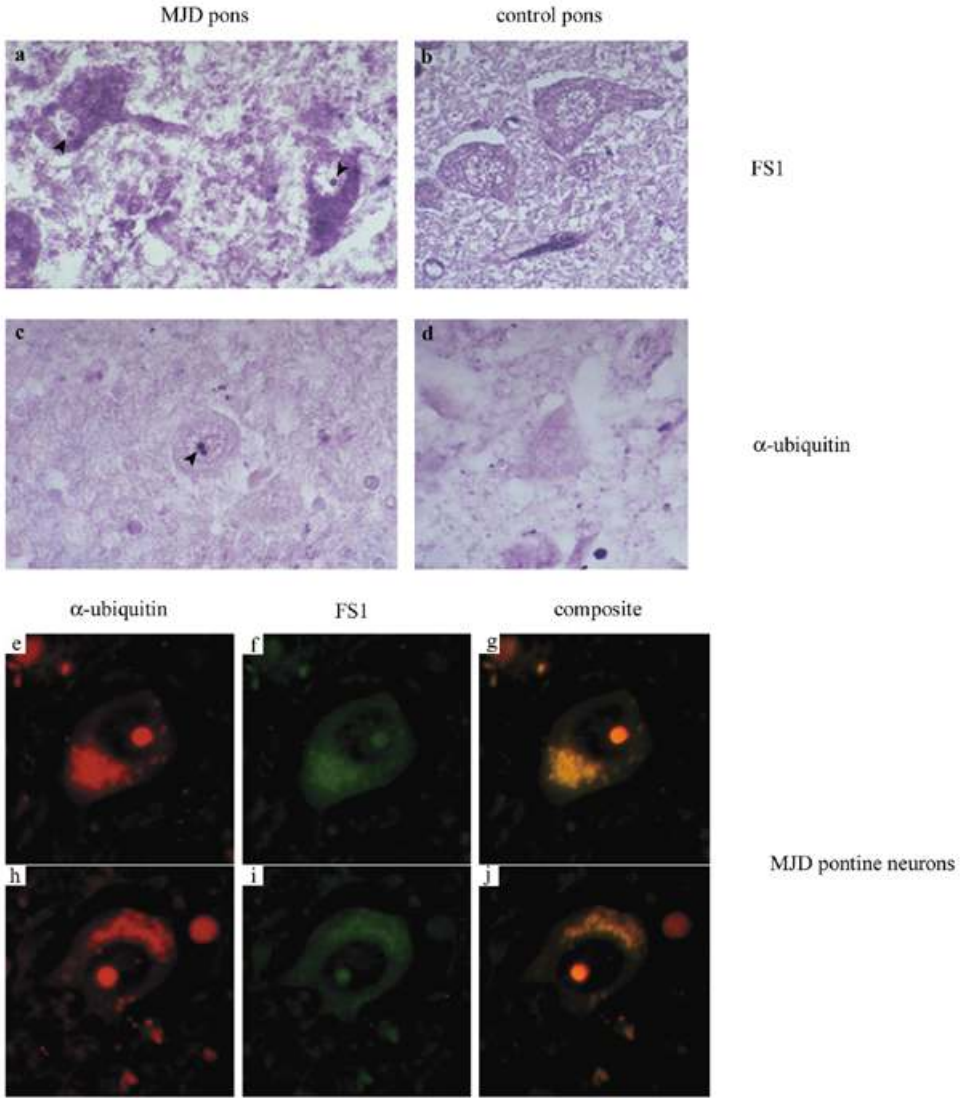

Figure 3. Immunohistochemical detection of INIs in MJD pontine neurons. Immunoprobing with FS1 antiserum in MJD pons (**a**) and control pons (**b**); immunoprobing with anti-ubiquitin in MJD pons (**c**) and control pons (**d**). INIs in pontine neurons are indicated by arrowheads. Double labeling immunofluorescence analysis of MJD pons showing ubiquitin-labeled INIs (**e** and **h**) and FS1-labeled INIs (**f** and **1**), and the composite image of both labelings (**g** and **j**). For all panels, the magnification before publication is 1000×, before reproduction.

constructs in which the reading frame immediately before the CAG repeat was mutated to code for a polyalanine stretch. These constructs, pMJD9 and pMJD10, contained stretches of 14 and 82 GCA repeats, respectively, and were fused in-frame to the *EGFP* gene (Fig. 4). We also added an HA tag at the C-terminus in-frame with the GCA stretch. COS-7 cells were transfected with these constructs, and with pMJD7 and pMJD8, which contained 14 and 82 CAG repeats, respectively, as well as *EGFP* fused in-frame with the CAG tracts. In addition, an HA epitope was also added at the C-terminus in-frame with the GCA tracts, and so only detectable if frameshifts occurred (Fig. 4). The addition of this independent, well characterized epitope to the constructs will also allow us to address the possibility that the high molecular weight products, INIs and green fluorescence detected in Figures 1, 2, 3 and 5 come from the unknown 83 kDa protein detected by the FS1 and FS2 antisera.

In a time-course experiment using anti-HA antibody as a probe to detect only protein frameshifted to the alanine frame, we collected and immunostained cells at 8, 12, 16, 20, 24, 48 and 72 h. Cells transfected with the CAG/Gln constructs pMJD7 and pMJD8 showed faint background staining at 8 h (Fig. 6a and c). Positive signal was detected for these two constructs at 12 h (data not shown) in the form of INIs (typically one or two per nucleus). At 20 h, nuclei of cells transfected with pMJD7 and pMJD8 contained inclusions, but were morphologically normal (Fig. 6f and h). At 24 h, cells transfected with the shorter construct remained morphologically normal (Fig. 6k), but cells transfected with the construct bearing 82 CAG repeats started showing some perinuclear and cytoplasmic inclusions in addition to the intranuclear aggregates (Fig. 6m). At this time-point ~85% of transfected cells have HA-positive inclusions when transfected with pMJD8, whereas only 40% of transfected cells show inclusions when

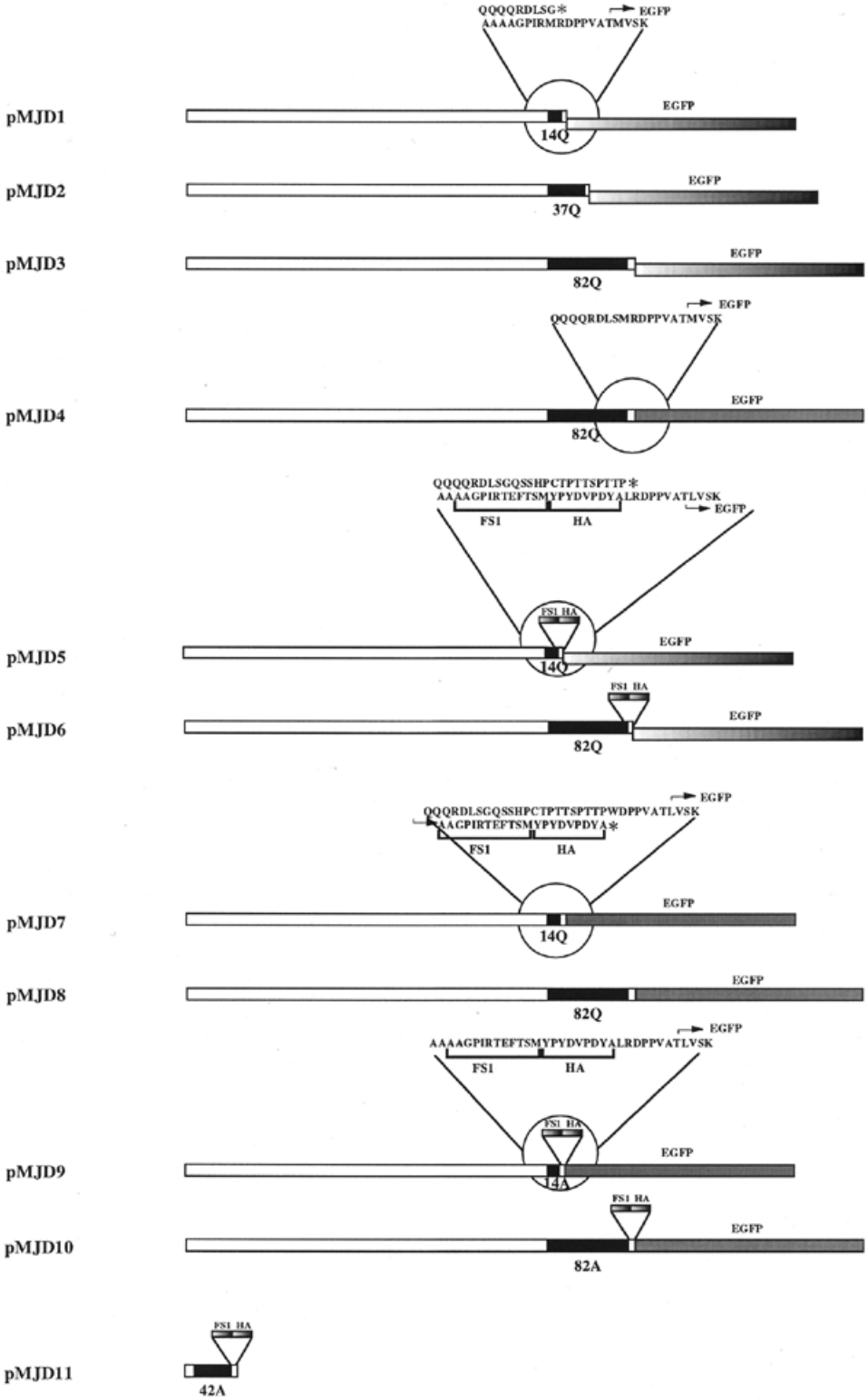

Figure 4. Constructs used in the transfection experiments. All constructs, with the exception of pMJD11, represent full-length *MJD-1*. Solid black boxes indicate the repeat portion of the constructs. Staggered ends indicate that EGFP will only be expressed if a frameshift occurs. The encircled enlarged detail of pMJD1 is also present in pMJD2 and pMJD3; details of pMJD5 are present in pMJD6; details of pMJD7 are present in pMJD8 and details of pMJD9 are the same as those in pMJD10.

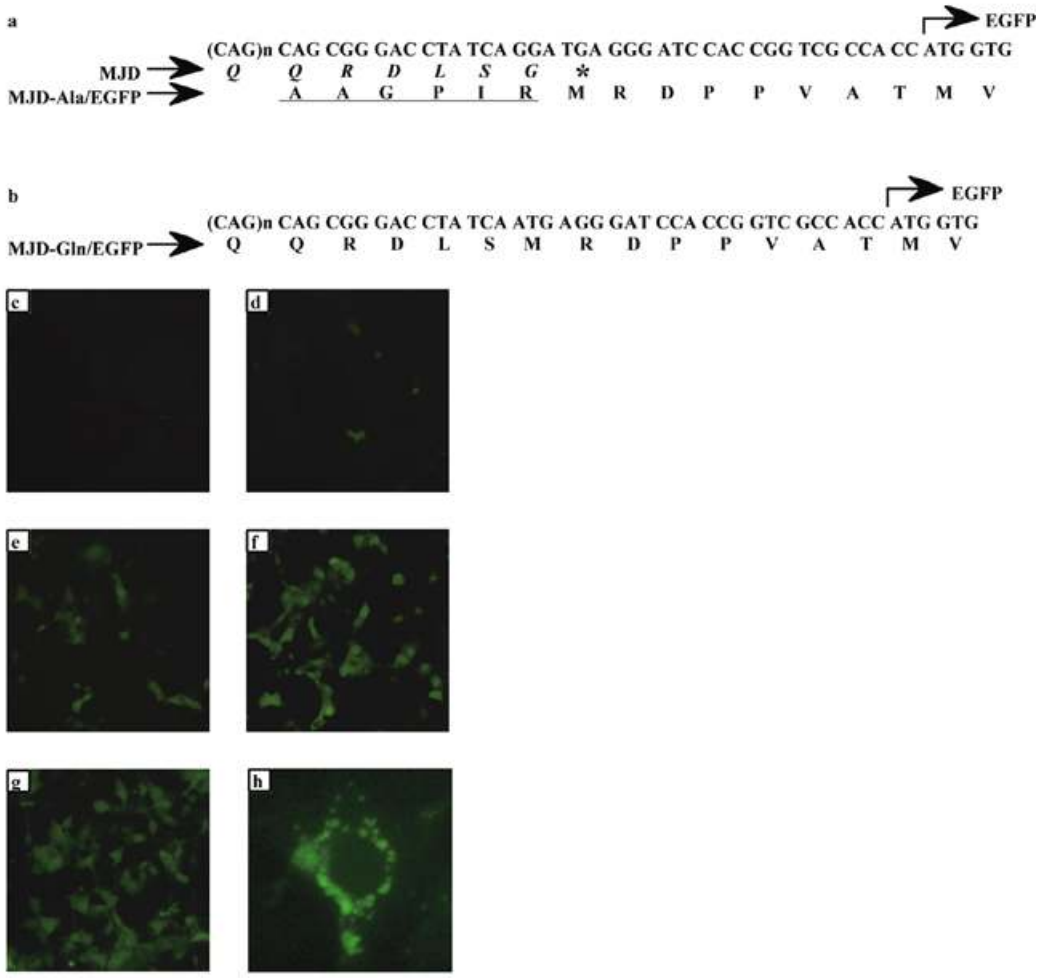

Figure 5. Transfection experiments with different MJD/EGFP constructs. (**a**) DNA sequence of the clones with *EGFP* out of frame (pMJD1, pMJD2 and pMJD3) and (**b**) with *EGFP* in glutamine frame (pMJD4), both (a and b) showing the predicted amino acid sequence. (**c–e**) Fluorescence at 72 h of COS-7 cells transfected with pMJD1 (c), pMJD2 (d) and pMJD3 (e) where the MJD$(CAG)_n$EGFP fusion protein is translated only when frameshifts to GCA-polyAla occur. (**f**) COS-7 cells transfected with pMJD4 where EGFP is in frame with CAG-Gln. (**g**) COS-7 cells transfected with the vector pEGFP-N1. (**h**) Perinuclear fluorescent aggregates observed in cells transfected with pMJD3. Pictures of sections in (c)–(g) were taken at 25× magnification for a fixed exposure time of 60 s before reproduction; picture in (h) is at 400× before reproduction.

transfected with pMJD7, suggesting that frameshifts occur with both constructs, but more frequently for the longer repeat. Nuclei of cells stained at 48 h showed some membrane disintegration with both constructs, but cells containing the longer CAG repeat also had perinuclear and cytoplasmic inclusions (Fig. 6p and r), indicating a more severe phenotype. It is useful to reiterate that probing cells transfected with the CAG/Gln constructs with anti-HA will only detect frameshifted protein. These species are detected early in the transfection and only as INIs, suggesting that, despite the probable rarity of frameshifts, they are producing proteins that accumulate as insoluble INIs.

We detected inclusions for both GCA/Ala constructs (14A and 82A) as early as 8 h after transfection (Fig. 6b and d). Typically, cells have one major perinuclear or cytoplasmic inclusion and abnormal nuclear morphology. The cellular phenotype progresses rapidly with time in cells transfected with either pMJD9 (Fig. 6g, l and q) or pMJD10 (Fig. 6i, n and s), and was extremely severe when compared with the CAG/Gln counterparts of the same repeat size (compare panels m and n in Fig. 6). Cells transfected with the GCA/Ala constructs show abnormal nuclear structure and aggregate formation mainly in the cytoplasm, usually with one major juxtanuclear inclusion and what appears to be cytoskeletal reorganization. Similar results were obtained in cells transfected in parallel with the same constructs but probed with FS1 antiserum (data not shown). At all time-points cells transfected with the pEGFP-N1 vector alone showed only background staining and were devoid of inclusions (Fig. 6e, j, o and t).

Western blots of protein extracted from the transfected cells were performed to investigate the nature of the inclusions found. Probing the blots with anti-HA detected a signal for both GCA/Ala constructs (pMJD9 and pMJD10), where the HA tag is in the main reading frame (Fig. 7a). No signal is detected with equivalent exposure for the CAG/Gln constructs, but overexposure of the blots reveals the presence of smears and protein in the wells for these constructs as well. In addition, whereas discrete bands are resolved with pMJD8, signal is only seen in the stacking gel with pMJD10, suggesting that the larger polyAla-containing proteins are very insoluble and do not migrate into the gel at all. Probing the same blots with 1C2

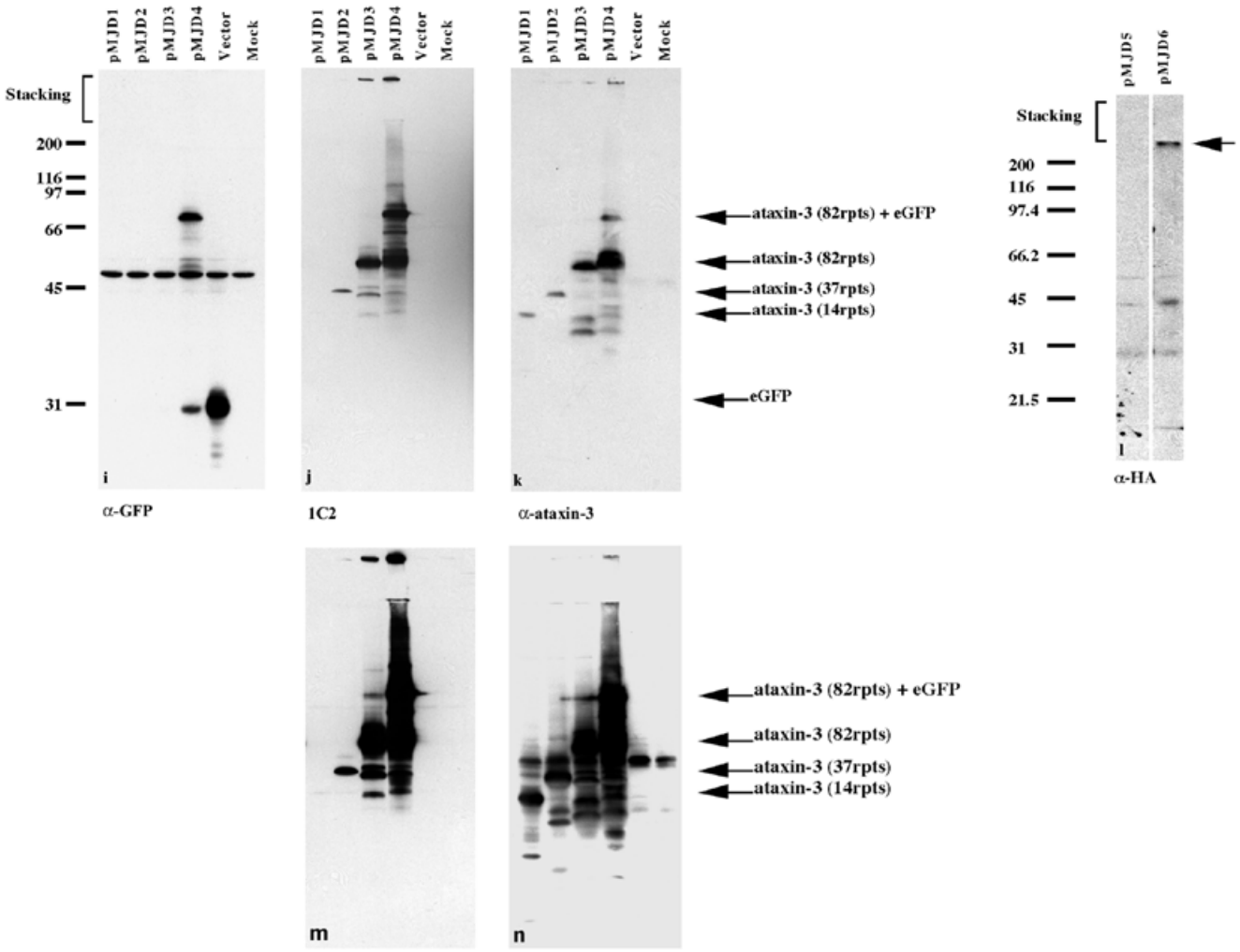

Figure 5. (*continued*) Transfection experiments with different MJD/EGFP constructs. (**i–l**) Western blots of protein isolated from cells shown in (c)–(g) and from mock transfected cells, immunoprobed with anti-GFP (**i**), 1C2 (**j**), anti-ataxin-3 (**k**) and anti-HA (**l**). (**m** and **n**) These panels represent overexposures of (j) and (k), respectively. Arrows on the right of (k) indicate the proteins detected. The arrowhead in (l) indicates threshold between stacking and resolving portions of the gel. Rpts, repeats.

confirms the presence of polyGln-containing proteins in the cells transfected with pMJD8, and the absence of such proteins in cells transfected with frameshifted constructs (Fig. 7b). The presence of signal in the stacking gel for pMJD8 may result from the presence of enough Gln residues to allow detection by the 1C2 antibody. It could also be due to the recruitment of the intact non-frameshifted protein into the insoluble aggregates, recruitment of hybrid polyAla/polyGln protein, or polyGln protein accumulation independent of polyAla polymers.

PolyGCA/polyAla stretches alone are sufficient for formation of aggregates

In order to determine whether a construct with only a GCA tract encoding an alanine peptide, outside the context of the ataxin-3 protein, would be sufficient to produce a cellular phenotype, we transfected a truncated $(GCA)_{42}$ construct with FS1 and HA epitopes in-frame with GCA into COS-7 cells (pMJD11, Fig. 4). In this construct we truncated the *MJD-1* sequence so that the resulting protein will only have 25 amino acid residues left upstream of the repeat, and only the FS1 and HA epitopes after the GCA tract. At 24 h, cells have perinuclear and cytoplasmic aggregates and nuclear morphology is abnormal (Fig. 8a), a phenotype that is very similar to the one obtained by transfection of the full-length GCA/Ala constructs described above. Mock transfected cells showed background staining and absence of inclusions (Fig. 8b). These findings indicate that the presence of a transgene expressing almost exclusively a polyAla tract is sufficient for formation of aggregates, independent of the protein context.

DISCUSSION

Our data are consistent with our hypotheses that frameshifts occur within CAG repeats to produce alanine-containing proteins, and that these proteins accumulate as aggregates. Detection of the hypothetical peptide in lymphoblastoid and neuronal cells of MJD patients and not in controls, and the production of green fluorescence preferentially in cells transfected with *MJD-1* bearing large CAG tracts with an out-of-frame EGFP, supports the occurrence of rare frameshifts

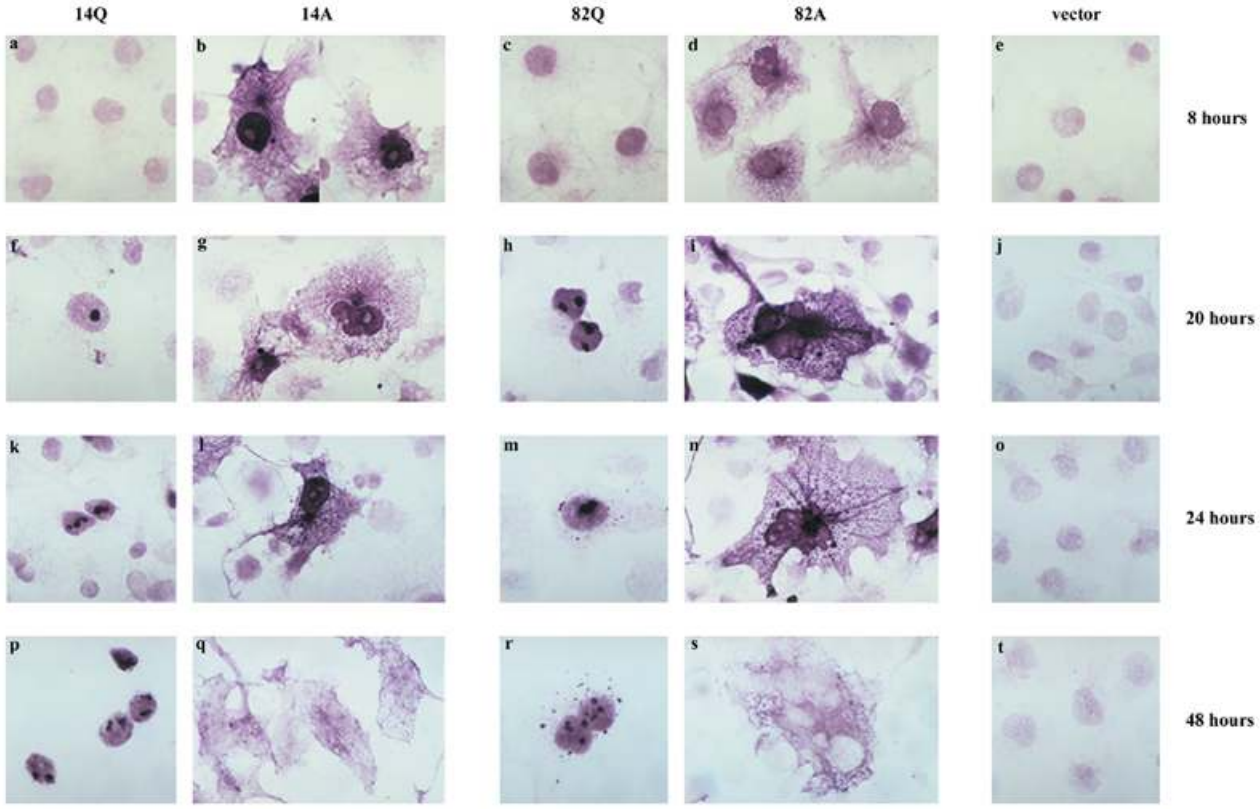

Figure 6. Time-course immunocytochemical analysis of COS-7 cells transfected with constructs encoding ataxin-3 with either a polyAla or a polyGln tract. Immunoprobing with anti-HA antibody at time-points 8 h: (**a**) pMJD7, (**b**) pMJD9, (**c**) pMJD8, (**d**) pMJD10 and (**e**) vector pEGFP-N1 alone; 20 h: (**f**) pMJD7, (**g**) pMJD9, (**h**) pMJD8, (**i**) pMJD10 and (**j**) vector pEGFP-N1 alone; 24 h: (**k**) pMJD7, (**l**) pMJD9, (**m**) pMJD8, (**n**) pMJD10 and (**o**) vector pEGFP-N1 alone; 48 h: (**p**) pMJD7, (**q**) pMJD9, (**r**) pMJD8, (**s**) pMJD10 and (**t**) vector pEGFP-N1 alone. For all panels pictures were taken at 1000× magnification, before reproduction.

during transcription and/or translation of long CAG tracts resulting from use of the alternative GCA/Ala reading frame. Additional experiments need to be conducted in order to better define the role of CAG tract length in frameshifting.

Slippage into the third possible frame, AGC/Ser, may also be occurring. However, the absence of diseases associated with tracts of polyserine and the physical nature of alanine polymers resulted in our exclusive focus on the GCA/Ala frame. Although the relative frequencies of different frameshifts remain unknown, the fact that most translational frameshift errors cause a +2 shift in the frame (20) suggests that GCA/Ala may be the more frequent of the mutant species.

Our data are also consistent with our contention that polyAla tracts are toxic and lead to the formation of INIs. We have also presented evidence that in cells transfected with the CAG/Gln constructs, frameshifting into the alanine frame is progressive, and frameshifted products are slowly accumulating in the nucleus as INIs (Fig. 5). Given the expected low frequency of frameshifts, our finding of frameshifted protein in INIs as early as 12 h after transfection argues that polyAla accumulation is a very early event in the formation of these structures. In fact, in cells transfected with as few as 14 CAGs, frameshifts are occurring and polyalanine-containing protein is accumulating in the nucleus as INIs. This finding is consistent with a recent report by Perez *et al*. (16) showing that transfection of normal sized CAG repeats leads to INIs. The absence of high molecular weight product for the 14 CAG construct in Figure 7 is also consistent with this report, and supports the possibility that inclusions formed by short repeats differ from those formed by expanded repeats, in that they would be more easily denatured and the protein would migrate into the gel. In contrast with the slow, progressive accumulation detected for the CAG/Gln constructs, transfection with the GCA/Ala constructs results in early and rapid accumulation of alanine-containing product. In this case the cells seem unable to cope with the presence of the protein, resulting in an earlier and much more severe phenotype. The sites of accumulation of polyAla products, consisting of one major juxtanuclear aggregate per cell and several smaller inclusions, are similar to the location of aggresomes, structures that form when the capacity of the proteasome degradation pathway is exceeded (17). These data seem to indicate that the direct expression of polyalanine in cells is likely to be poorly tolerated by the cell.

Recent reports seem to shed new light into the role of INIs in trinucleotide repeat diseases (18,19). In SCA1 transgenic mice, for instance, formation of aggregates in the nucleus is apparently not necessary for initiation of symptoms, and nuclear localization of the protein (and not only the presence of a CAG repeat) is important for pathogenesis in these mice (18). These important findings are equally applicable to our alanine toxicity model as to the glutamine toxicity model, and so remain consistent with our hypothesis.

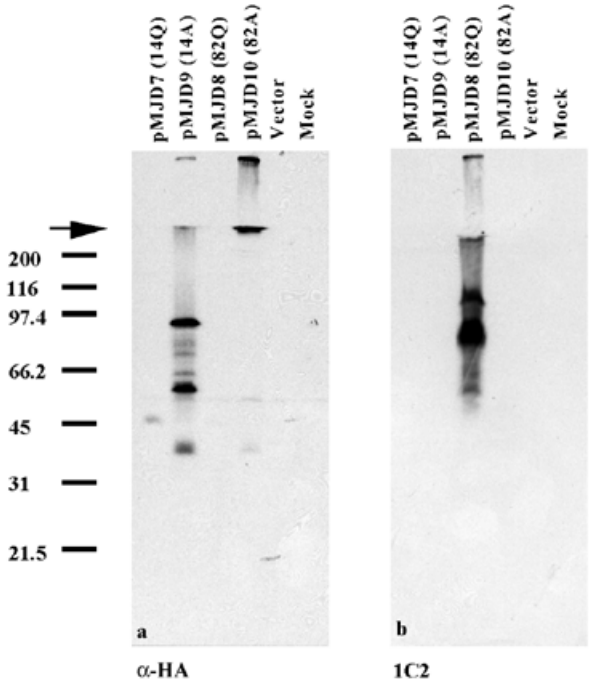

Figure 7. Western analysis of transfected COS-7 cells (in Fig. 5). Blots were probed with (**a**) anti-HA and (**b**) 1C2. The arrow indicates threshold between stacking and resolving portions of the gel. Cells were harvested at 72 h after transfection.

Although we have shown that polyAla tracts are harmful to cells, and provided evidence that, in exp-CAG tract MJD, frameshifted protein is produced and accumulates in the nucleus, we have not shown that these proteins have a role in disease pathogenesis. It may be that the frameshifted protein is recruited into INIs by the polyGln portion of the protein, or that these species are so infrequent as to be inconsequential to the cell. Additional work needs to be done to define the role, if any, of frameshifted protein in MJD and other exp-CAG tract disorders.

MATERIALS AND METHODS

Antisera production

A 12mer peptide corresponding to the new predicted C-terminus of the ataxin-3 protein after frameshift occurs (AAGPIRTEFTSM) was used to raise antisera from two rabbits, FS1 and FS2. Injections were performed using 0.5 mg of peptide conjugated to keyhole limpet hemacyanin protein carrier and sera were collected using standard protocols (21).

Western blots

For protein extraction, MJD and control lymphoblastoid cells were lysed in buffer containing NP-40. Equal amounts of protein were electrophoresed in 8% SDS–polyacrylamide gels and transblotted to nitrocellulose membranes. Immunodetection was performed using FS1 (1:300), FS2 (1:300), anti-ataxin-3 (1:1000), 1C2 (1:2000), anti-ubiquitin (1:400; Dako) and FS1 and FS2 pre-immune serum (1:300). Results for FS1 and FS2 were always consistent; all experiments were repeated three times on different blots. Horseradish peroxidase-conjugated secondary antibodies were used at a 1:10 000 dilution. COS-7 cells transfected with various constructs were collected, washed and lysed in sample loading buffer. One hundred micrograms of each sample was used to run on a 10% SDS–PAGE and transblotted onto nitrocellulose membranes. Immunodetection was performed using antisera at following dilutions: 1C2 (1:5000), anti-ataxin-3 (1:2000) and anti-HA (1:1000). Results were visualized by chemiluminescence (Renaissance).

Immunocytochemistry

MJD and control lymphoblastoid cells were harvested and a total of 5×10^5 cells from each cell line were plated onto poly-D-lysine coated slides and fixed with acetone/methanol (1:1). Immunodetection was performed using FS1 (1:300), anti-ubiquitin (1:300), anti-ataxin-3 (1:500) and FS1 pre-immune serum (1:300). Biotinylated secondary antibodies were used at a 1:500 dilution and an amplification step was performed using the ABC kit (Vector). Reaction product was visualized using the VIP kit (Vector).

Immunocytochemistry on COS-7 cells was performed on cover slips. At each time-point cells were fixed with 4% paraformaldehyde and immunodetection was performed using an anti-HA probe (1:500) and FS1 (1:300). Secondary antibodies and subsequent amplification and detection procedures were carried out as described above.

Immunohistochemistry

For immunohistochemistry of brain sections we used 5 µm sections of paraffin-embedded tissue from the pons of an MJD patient and a control subject. Sections were deparaffinized, permeabilized and immunostained with FS1 (1:50) and anti-

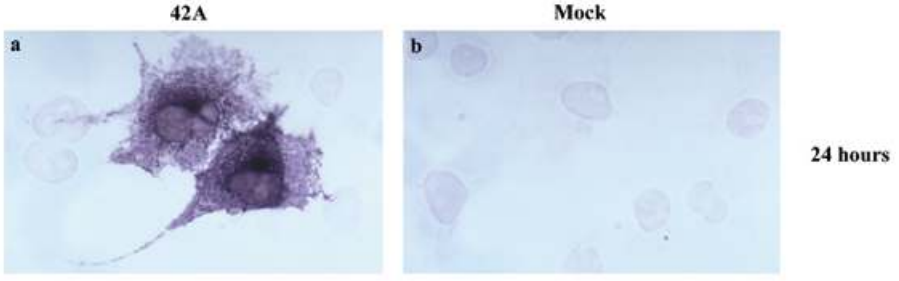

Figure 8. Immunocytochemical analysis of COS-7 cells transfected with a truncated polyAla-encoding construct. Immunoprobing with anti-HA antibody in: (**a**) cells transfected with 42A and (**b**) mock transfected cells. For all panels pictures were taken at 1000× magnification, before reproduction.

ubiquitin (1:300) (Dako). Biotinylated secondary antibodies were used at a 1:500 dilution and an amplification step was performed using the ABC kit (Vector). Reaction product was visualized using the VIP kit (Vector). For co-immunofluorescence of FS1 and anti-ubiquitin antibodies in brain sections, the same procedure for preparation of samples was followed. Immunodetection was performed using FS1 (1:50) and monoclonal anti-ubiquitin (Zymed) (1:300). A mixture of Cy3-conjugated anti-mouse antibody (1:100) and fluorescein-conjugated anti-rabbit antibody (1:50) was used as secondary probe. Sections were mounted in SlowFade (Molecular Probes).

Plasmid construction, transfection and cell culture

DNA amplification was performed using Pfu DNA polymerase (Stratagene, La Jolla, CA). Primer MJD-5′ (5′-TTTTAAGCTTAGACAAATAAACATGGAG-3′) was used in conjunction with MJD-3′ (5′-CCGGTGGATCCCTCATCCTGATAGGTCCCGCTGCTG-3′) for pMJD1, pMJD2 and pMJD3, or MJD-3′c (5′-CCGGTGGATCCCTCATTGATAGGTCCCGCTGCTG-3′) for pMJD4 (Stratagene). Primer MJD-5′(HIII) (5′-TTTTAAGCTTCCCACCATGGAGTCCATCTTCCA-3′) was used in conjunction with MJD-3′(BI) (5′-CCGGTGGATCCCTCAGGGCGTAGTCGGGGACGTCGTAGGGGTACATGGATGTGAACTCTGTCCTGATAGGTCCCGCTG-3′). For pMJD5 and pMJD6, or MJD-3′c(BI) (5′-CCGGTGGATCCCAGGGCGTAGTCGGGGACGTCGTAGGGGTACATGGATGTGAACTCTGTCCTGATAGGTCCCGCTG-3′) for pMJD7 and pMJD8, or MJD-Ala (5′-CGGAAGAGACGAGAAGCCTACTCCGGAAAAACAGCAGCAAAAGCAGC-3′) for pMJD9, pMJD10 and pMJD11. Amplified products were digested with *Bam*HI and *Hin*dIII and cloned into plasmid pEGFP-N1 (Clontech, Palo Alto, CA**??**), except for pMJD11, where the amplified product was cloned into a modified version of the pEGFP-N1 plasmid lacking the *EGFP* gene. All constructs were confirmed by sequencing. COS-7 cells were seeded in Dulbecco's modified Eagle's medium containing 10% fetal calf serum the day before transfection at 2×10^5 per well in six-well plates containing sterile coverslips. COS-7 cells were transfected with plasmid DNA (2.0 μg) using Lipofectamine reagent (Gibco BRL) according to the manufacturer's instructions. For the experiment depicted in Figure 4, after 72–96 h, the cells were fixed with phosphate-buffered saline/4% paraformaldehyde and observed under a fluorescence microscope with FITC filter in four independent experiments.

ACKNOWLEDGEMENTS

We would like to thank H.L. Paulson for sharing the anti-ataxin-3 antibody, Jun Goto for the *MJD-1* cDNA, S. Hayes, S. Kaan, N. Chrétien, D. Rochefort, J. Parboosingh, A. Toulouse and V. Shanmugam for useful discussion and review of the manuscript, and Y. Robitaille for providing the MJD pathological material. B.B. is a chercheur-boursier of the Fonds de Recherches en Santé du Québec, C.G. is the recipient of a scholarship from JNICT (Praxis XXI) Portugal and G.A.R. is supported by the Medical Research Council of Canada.

REFERENCES

1. Kawaguchi, Y., Okamoto, T., Taniwaki, M., Aizawa, M., Inoue, M., Katayama, S., Kawakami, H., Nakamura, S., Nishimura, M., Akiguchi, I. *et al.* (1994) CAG expansions in a novel gene for Machado-Joseph disease at chromosome 14q32.1. *Nature Genet.*, **8**, 221–228.
2. Hardy, J. and Gwinn-Hardy, K. (1998) Genetic classification of primary neurodegenerative disease. *Science*, **282**, 1075–1079.
3. Paulson, H.L., Perez, M.K., Trottier, Y., Trojanowski, J.Q., Subramony, S.H., Das, S.S., Vig, P., Mandel, J.L., Fischbeck, K.H. and Pittman, R.N. (1997) Intranuclear inclusions of expanded polyglutamine protein in spinocerebellar ataxia type 3. *Neuron*, **19**, 333–344.
4. Davies, S.W., Turmaine, M., Cozens, B.A., DiFiglia, M., Sharp, A.H., Ross, C.A., Scherzinger, E., Wanker, E.E., Mangiarini, L. and Bates, G.P. (1997) Formation of neuronal intranuclear inclusions underlies the neurological dysfunction in mice transgenic for the HD mutation. *Cell*, **90**, 537–548.
5. Ordway, J.M., Tallaksen-Greene, S., Gutekunst, C.A., Bernstein, E.M., Cearley, J.A., Wiener, H.W., Dure, L.S.I., Lindsey, R., Hersch, S.M., Jope, R.S. *et al.* (1997) Ectopically expressed CAG repeats cause intranuclear inclusions and a progressive late onset neurological phenotype in the mouse. *Cell*, **91**, 753–763.
6. Skinner, P.J., Koshy, B.T., Cummings, C.J., Klement, I.A., Helin, K., Servadio, A., Zoghbi, H.Y. and Orr, H.T. (1997) Ataxin-1 with an expanded glutamine tract alters nuclear matrix-associated structures. *Nature*, **389**, 971–974.
7. Davies, S.W., Beardsall, K., Turmaine, M., DiFiglia, M., Aronin, N. and Bates, G.P. (1998) Are neuronal intranuclear inclusions the common neuropathology of triplet-repeat disorders with polyglutamine-repeat expansions? *Lancet*, **351**, 131–133.
8. Brais, B., Bouchard, J.P., Xie, Y.G., Rochefort, D.L., Chretien, N., Tome, F.M., Lafreniere, R.G., Rommens, J.M., Uyama, E., Nohira, O. *et al.* (1998) Short GCG expansions in the PABP2 gene cause oculopharyngeal muscular dystrophy. *Nature Genet.*, **18**, 164–167.
9. Blondelle, S.E., Forood, B., Houghten, R.A. and Perez-Paya, E. (1997) Polyalanine-based peptides as models for self-associated beta-pleated-sheet complexes. *Biochemistry*, **36**, 8393–8400.
10. Forood, B., Perez-Paya, E., Houghten, R.A. and Blondelle, S.E. (1995) Formation of an extremely stable polyalanine beta-sheet macromolecule. *Biochem. Biophys. Res. Commun.*, **211**, 7–13.
11. van Leeuwen, F.W., de Kleijn, D.P., van den Hurk, H.H., Neubauer, A., Sonnemans, M.A., Sluijs, J.A., Koycu, S., Ramdjielal, R.D.J., Salehi, A., Martens, G.J.M. *et al.* (1998) Frameshift mutants of beta amyloid precursor protein and ubiquitin-B in Alzheimer's and Down patients. *Science*, **279**, 242–247.
12. Linton, M.F., Raabe, M., Pierotti, V. and Young, S.G. (1997) Reading-frame restoration by transcriptional slippage at long stretches of adenine residues in mammalian cells. *J. Biol. Chem.*, **272**, 14127–14132.
13. Kurland, C. and Gallant, J. (1996) Errors of heterologous protein expression. *Curr. Opin. Biotechnol.*, **7**, 489–493.
14. Paulson, H.L., Das, S.S., Crino, P.B., Perez, M.K., Patel, S.C., Gotsdiner, D., Fischbeck, K.H. and Pittman, R.N. (1997) Machado-Joseph disease gene product is a cytoplasmic protein widely expressed in brain. *Ann. Neurol.*, **41**, 453–462.
15. Trottier, Y., Lutz, Y., Stevanin, G., Imbert, G., Devys, D., Cancel, G., Saudou, F., Weber, C., David, G., Tora, L. *et al.* (1995) Polyglutamine expansion as a pathological epitope in Huntington's disease and four dominant cerebellar ataxias. *Nature*, **378**, 403–406.
16. Perez, M.K., Paulson, H.L., Pendse, S.J., Saionz, S.J., Bonini, N.M. and Pittman, R.N. (1998) Recruitment and the role of nuclear localization in polyglutamine-mediated aggregation. *J. Cell Biol.*, **143**, 1457–1470.
17. Johnston, J.A., Ward, C.L. and Kopito, R.R. (1998) Aggresomes: a cellular response to misfolded proteins. *J. Cell Biol.*, **143**, 1883–1898.
18. Klement, I.A., Skinner, P.J., Kaytor, M.D., Yi, H., Hersch, S.M., Clark, H.B., Zoghbi, H.Y. and Orr, H.T. (1998) Ataxin-1 nuclear localization and aggregation—role in polyglutamine-induced disease in SCA1 transgenic mice. *Cell*, **95**, 41–53.
19. Saudou, F., Finkbeiner, S., Devys, D. and Greenberg, M.E. (1998) Huntingtin acts in the nucleus to induce apoptosis but death does not correlate with the formation of intranuclear inclusions. *Cell*, **95**, 55–66.
20. Farabaugh, P.J. (1996) Programmed translational frameshifting. *Ann. Rev. Genet.*, **30**, 507–528.
21. Harlow, E. and Lane, D. (1988) *Antibodies*. Cold Spring Harbor Laboratory Press, Cold Spring Harbor, NY.

Figure 1. Western blot analysis of lymphoblastoid cells from controls and MJD patients. (**a**) Schematic representation of the MJD-Ala protein that results from a frameshift in the CAG tract showing the new C-terminus (italicized; used to raise the FS1 and FS2 antibodies). (b–e) Western blots of two control lymphoblastoid cell lines (cLCL) and four MJD lymphoblastoid cell lines (MJDLCL) immunoprobed with FS1 (**b**), anti-ataxin-3 (**c**), 1C2 (**d**) and FS1 pre-immune serum (**e**). The arrow indicates the threshold between stacking and resolving portions of the gel. (b)–(d) represent serial probing of a single membrane.

Figure 2. Immunocytochemical detection of intranuclear deposits in lymphoblastoid cells. Immunocytochemistry of control LCL versus MJD LCL: absence of INIs in control LCL probed with FS1 (**a**), with anti-ubiquitin (**c**), and detection of INIs in MJD LCL with FS1 (**b**) and anti-ubiquitin (**d**). (**e**) Immuno-detection of MJD LCL with FS1 pre-immune serum. For all panels, the magnification before publication is 400× (left) and 1000× (right). These results have been replicated in three separate experiments.

Figure 3. Immunohistochemical detection of INIs in MJD pontine neurons. Immunoprobing with FS1 antiserum in MJD pons (**a**) and control pons (**b**); immunoprobing with anti-ubiquitin in MJD pons (**c**) and control pons (**d**). INIs in pontine neurons are indicated by arrowheads. Double labeling immunofluorescence analysis of MJD pons showing ubiquitin-labeled INIs (**e** and **h**) and FS1-labeled INIs (**f** and **1**), and the composite image of both labelings (**g** and **j**). For all panels, the magnification before publication is 1000×, before reproduction.

Figure 4. Constructs used in the transfection experiments. All constructs, with the exception of pMJD11, represent full-length *MJD-1*. Solid black boxes indicate the repeat portion of the constructs. Staggered ends indicate that EGFP will only be expressed if a frameshift occurs. The encircled enlarged detail of pMJD1 is also present in pMJD2 and pMJD3; details of pMJD5 are present in pMJD6; details of pMJD7 are present in pMJD8 and details of pMJD9 are the same as those in pMJD10.

Figure 5. Transfection experiments with different MJD/EGFP constructs. (**a**) DNA sequence of the clones with *EGFP* out of frame (pMJD1, pMJD2 and pMJD3) and (**b**) with *EGFP* in glutamine frame (pMJD4), both (a and b) showing the predicted amino acid sequence. (**c–e**) Fluorescence at 72 h of COS-7 cells transfected with pMJD1 (c), pMJD2 (d) and pMJD3 (e) where the MJD$(CAG)_n$–EGFP fusion protein is translated only when frameshifts to GCA-polyAla occur. (**f**) COS-7 cells transfected with pMJD4 where EGFP is in frame with CAG-Gln. (**g**) COS-7 cells transfected with the vector pEGFP-N1. (**h**) Perinuclear fluorescent aggregates observed in cells transfected with pMJD3. Pictures of sections in (c)–(g) were taken at 25× magnification for a fixed exposure time of 60 s before reproduction; picture in (h) is at 400× before reproduction. (**i–l**) Western blots of protein isolated from cells shown in (c)–(g) and from mock transfected cells, immunoprobed with anti-GFP (**i**), 1C2 (**j**), anti-ataxin-3 (**k**) and anti-HA (**l**). (**m** and **n**) These panels represent overexposures of (j) and (k), respectively. Arrows on the right of (k) indicate the proteins detected. The arrowhead in (l) indicates threshold between stacking and resolving portions of the gel. Rpts, repeats.

Figure 6. Time-course immunocytochemical analysis of COS-7 cells transfected with constructs encoding ataxin-3 with either a polyAla or a polyGln tract. Immunoprobing with anti-HA antibody at time-points 8 h: (**a**) pMJD7, (**b**) pMJD9, (**c**) pMJD8, (**d**) pMJD10 and (**e**) vector pEGFP-N1 alone; 20 h: (**f**) pMJD7, (**g**) pMJD9, (**h**) pMJD8, (**i**) pMJD10 and (**j**) vector pEGFP-N1 alone; 24 h: (**k**) pMJD7, (**l**) pMJD9, (**m**) pMJD8, (**n**) pMJD10 and (**o**) vector pEGFP-N1 alone; 48 h: (**p**) pMJD7, (**q**) pMJD9, (**r**) pMJD8, (**s**) pMJD10 and (**t**) vector pEGFP-N1 alone. For all panels pictures were taken at 1000× magnification, before reproduction.

Figure 7. Western analysis of transfected COS-7 cells (in Fig. 5). Blots were probed with (**a**) anti-HA and (**b**) 1C2. The arrow indicates threshold between stacking and resolving portions of the gel. Cells were harvested at 72 h after transfection.

Figure 8. Immunocytochemical analysis of COS-7 cells transfected with a truncated polyAla-encoding construct. Immunoprobing with anti-HA antibody in: (**a**) cells transfected with 42A and (**b**) mock transfected cells. For all panels pictures were taken at 1000× magnification, before reproduction.